

Computational study of some heterocyclic compounds as corrosion inhibitors for aluminum using the DFT method

Abstract

DFT Calculations were performed on Oxazole, Pyrazole, Imidazole, Isoxazole, Thiazole and Isothiazole as corrosion inhibitors for aluminum with full optimization of geometries in DFT-B3LYP/6-31 G*Level (D, P) to find a relation between the molecular structure and corrosion inhibition. The electronic properties such as the energy of the highest occupied molecular orbital (HOMO), the energy of lowest unoccupied orbital (LUMO), the energy gap (LUMO–HOMO), quantum chemical parameters such as hardness, softness, the fraction of the electron transferred, and the electrophilicity index. In order to know the relationship of molecular structure and corrosion inhibition on surface of the Quantum chemical parameters, boundary orbital's isothiazole has been found the highest anti-corrosion efficiency as compared to other

Keywords :Al , DFT, Corrosion, heterocyclic compounds, inhibitor

Introduction

Aluminum is widely used as a material in automobiles, aviation, household appliances, containers, and electronic devices [1,2]. The resistance of aluminum against corrosion in aqueous media can be attributed to the rapid formation of oxide films on the surface. However, aluminum gets easily corroded in the presence of corrosive acids [1,2]. Studies of the corrosion behavior of aluminum in different aggressive environments have continued to attract attention because of its important applications. Hydrochloric acid is one of the most widely used agents in the industrial sector and it corrodes metals such as aluminum. As such, there is a need to use inhibitors for retardation of the metal dissolution process [3]. Among several techniques used in mitigating corrosion problems, the use of chemical inhibitors remains the most cost-effective and practical method [4]. The development of aluminum corrosion inhibitors based on organic compounds is of growing interest in the field of corrosion chemistry [5]. The reason for this is that even though inorganic substances like phosphates, chromates, dichromates

and arsenates, were found to be effective as metal corrosion inhibitors, the major disadvantage is their toxicity and as such, their use has come under severe criticism [6]. Research has shown that organic inhibitors are viable and highly beneficial because they

are efficient, environmentally benign and comparatively cheap [7–8] and are more effective than inorganic compounds [9].

Computational methods:

Theoretical calculations of the quantum chemical parameters were performed with complete geometry optimizations using the standard Gaussian-09 software package³⁹. Geometry optimizations were carried out using B3LYP functional at the 6-31G* (d,p) basis set and at the density functional theory (DFT) level.

Results and Discussion

The inhibition efficiency of the could some heterocyclic compounds be determined from the quantum chemical parameters calculated from the optimized structure. These global parameters include the frontier Molecular Orbital's : E_{HOMO} (the highest occupied molecular orbital) and E_{LUMO} (the lowest unoccupied molecular orbital); the energy gap (ΔE_{gap}) between E_{HOMO} and E_{LUMO} ; the global hardness (η) of the inhibitor; the softness (σ); the fraction of the electron transferred (ΔN); the electrophilicity index (ω) of the

The inhibition efficiency of the could some heterocyclic compounds be determined from the quantum chemical parameters calculated from the optimized structure. These global parameters include the frontier Molecular Orbital's on Al According to Koopman's theorem[10] , the absolute electronegativity (χ), the absolute hardness (η), the softness (σ) and the electrophilicity index (ω) are given as follow[11]:

$$\omega = \frac{\mu^2}{2\eta} \quad , \quad (\mu = -\chi)$$

$$\chi = \frac{I+A}{2} \quad , \quad \chi = -\frac{E_{\text{HOMO}}+E_{\text{LUMO}}}{2}$$

$$\eta = \frac{I-A}{2} \quad , \quad \eta = -\frac{E_{\text{HOMO}}-E_{\text{LUMO}}}{2}$$

$$\sigma = 1/\eta$$

where the ionization potential (I) and the electron affinity (E) are calculated using the following relations according to the Molecular Orbital theory:

$$I = -E_{\text{HOMO}} \quad , \quad A = -E_{\text{LUMO}}$$

$$\Delta E_{(\text{gap})} = E_{\text{LUMO}} - E_{\text{HOMO}}$$

The chemical potential (μ) is assumed to be equal to the negative of the absolute electronegativity (χ). The electrophilic power (ω) of an inhibitor was proposed by Parr. [12] Herein, electrons flow from the less electronegative inhibitor (χ_{inh}) to higher electronegative Aluminum (χ_{Al}) until the chemical potentials become equal. The number of transferred electrons from the inhibitor to the metallic surface (ΔN) was also calculated from the obtained values of χ and η as follow[13]:

$$\Delta N = \frac{\chi_{Al} - \chi_{inh}}{2(\eta_{Al} + \eta_{inh})}$$

where χ_{Al} and χ_{inh} denote the absolute electronegativity and η_{Al} and η_{inh} denote the absolute hardness of Al and the inhibitor, respectively. The difference in electronegativity ($\chi_{Al} - \chi_{inh}$) drives the electron transfer, and ($\eta_{Al} + \eta_{inh}$) acts as resistance[14] . In this study, the theoretical values of $\chi_{Al} = 3.2093\text{eV}$ and $\eta_{Al} = 2.7764\text{eV}$ were used to calculate the number of electrons transferred[15] . All calculations have been performed for the molecules in the gas phase.

The frontier Molecular Orbital's (FMO) of the inhibitors shows the adsorbing ability of the molecule over metal surfaces [16] . E_{HOMO} indicates the capability of a molecule to donate electrons to the appropriate acceptor level of inhibitor with unoccupied d-orbital's of metal. E_{LUMO} indicates its ability to accept electrons. So, the lower E_{LUMO} value shows the higher ability of the molecule to accept electrons leading to better inhibitor efficiency[17] . Therefore, with increasing the HOMO energy and decreasing the LUMO energy the binding capability of the inhibitor to the metal surface increases.

Table 1. The calculated (HOMO-LUMO) energies of the inhibitors by DFT method.

Compounds	HOMO	LUMO
Al	-5.9857*	-0.4328*
Imidazole	-6.3598	0.6522
Pyrazole	-6.7286	0.3806
Oxazole	-7.2616	-0.4745
Isoxazole	-7.5438	-0.9140
Thiazole	-7.1346	-1.0492
Isothiazole	-7.2614	-1.2841

1 Hartree = 27.21160665 eV

[18] *

According to the frontier molecular orbital (FMO) theory, the chemical reactivity is a function of the interaction between the HOMO and LUMO levels of the reacting species [19,20] E_{HOMO} is a quantum chemical parameter which is associated with the electron donating ability of the molecule. A high value of E_{LUMO} is likely to indicate a tendency of the molecule of low empty molecular orbital energy [21]. The energy of the lowest unoccupied molecular orbital, E_{LUMO} , indicates the ability of the molecule to accept electrons [22]. So the lower the value of E_{LUMO} , the more the molecule accepts electrons. Thus the binding ability of the inhibitor to the metal surface increases with increasing HOMO and decreasing LUMO energy values.

Table 2: The calculated HOMO-LUMO gap interaction of Al with the inhibitors.

Inhibitors	$(\text{LUMO})_{\text{Inh}} - (\text{HOMO})_{\text{Al}}$ (eV)	$(\text{LUMO})_{\text{Al}} - (\text{HOMO})_{\text{Inh}}$ (eV)
Imidazole	6.6379	05.927
Pyrazole	6.3663	6.2958
Oxazole	5.5112	6.8288
Isoxazole	5.0717	07.111
Thiazole	4.9365	6.7018
Isothiazole	4.7016	6.8286

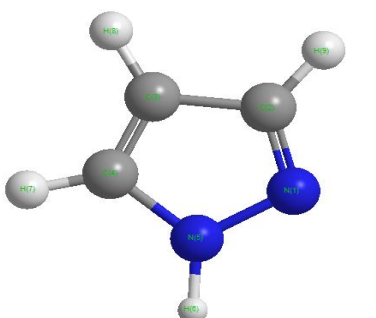
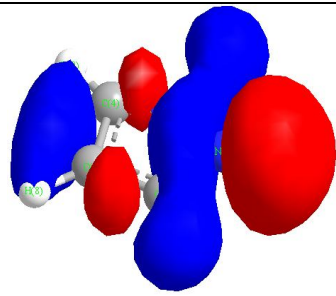
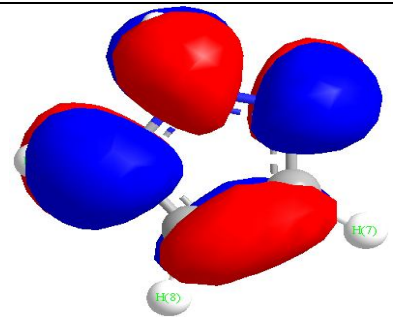
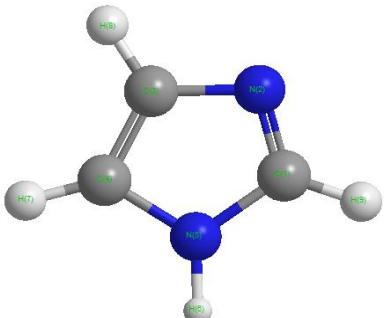
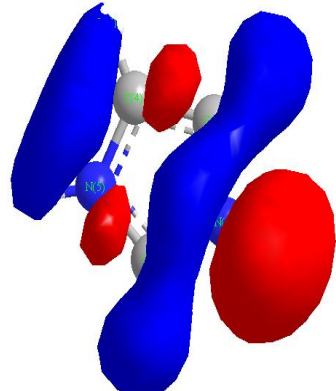
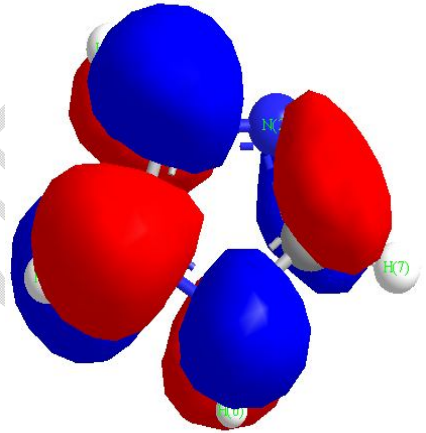
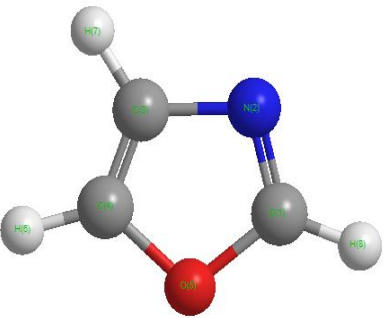
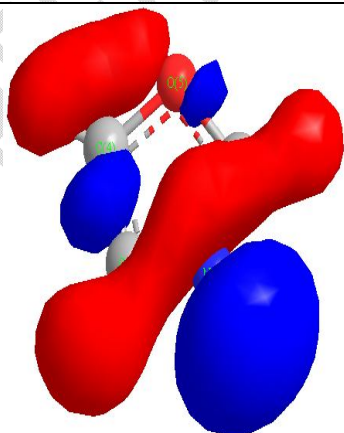
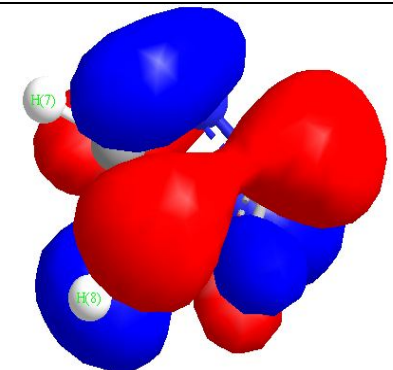
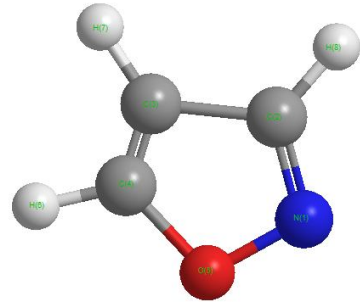
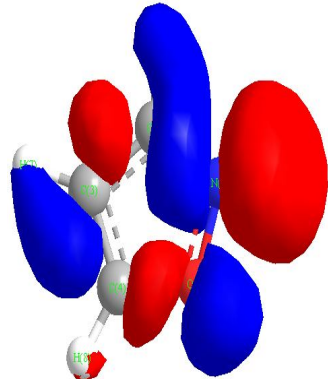
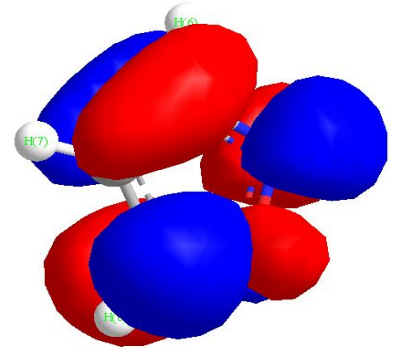
From Table 2, it can be seen that will Aluminum act as a Lewis base while the inhibitors Isoxazole , Thiazole and Isothizole act as a Lewis acids So Aluminum will utilize the HOMO to initiate the reaction with the LUMO orbital of the Isoxazole , Thiazole and Isothizole The interaction will have a certain amount of ionic character because the values of the $\text{LUMO}_{\text{inh}} - \text{HOMO}_{\text{Al}}$ gap approximately fall between 4 and 5 eV . A strong covalent bond can be expected only if the $\text{LUMO}_{\text{inh}} - \text{HOMO}_{\text{Al}}$ gap is approximately zero [23,24]. while Oxazole, Pyrazole, Imidazole inhibitors act as a base Lewis and aluminum as Lewis acid.

Thus Isoxazole, Thazole, Isothizole act as a cathodic inhibitor while Oxazole, Pyrazole, Imidazole act as an anodic inhibitor Table 3 show the calculated global reactivity parameters which were used to study the effectiveness of the inhibitors. These parameters include the electronegativity (χ), The global hardness (η), the global softness (σ), the fraction of electron transferred (ΔN), and the electrophilicity index (ω) of the molecules.

The values of ΔN show the inhibition efficiency resulting from electron donation by the aluminum inhibitor [25] The inhibition efficiency increases by increasing the ability of these inhibitors to donate electrons to the metal and the bulk of the transferred electrons are associated with the best inhibitor, and (ω) indicates the ability of the inhibitor to accept electrons of aluminum.

Figure1: HOMO & LUMO of the optimized fragments

inhibitor	Structure	HOMO	LUMO
-----------	-----------	------	------

<p>Pyrazole</p>	 <p>Ball-and-stick model of Pyrazole (1,2-diazole). The structure shows a five-membered aromatic ring with two adjacent nitrogen atoms (blue) and three carbon atoms (grey). Hydrogen atoms (white) are attached to the carbon atoms. Labels include N(1), N(2), C(3), C(4), C(5), H(3), H(4), and H(5).</p>	 <p>Electrostatic potential map of Pyrazole. Red regions indicate electron-rich areas (negative potential), and blue regions indicate electron-poor areas (positive potential). The map shows high electron density on the nitrogen atoms and the C3-C4 bond.</p>	 <p>Orbital density map of Pyrazole. The map shows the distribution of electron density in the molecule, with red and blue lobes representing different phases of the orbitals. Labels include H(3) and H(7).</p>
<p>Imidazole</p>	 <p>Ball-and-stick model of Imidazole (1H-imidazole). The structure shows a five-membered aromatic ring with two adjacent nitrogen atoms (blue) and three carbon atoms (grey). Hydrogen atoms (white) are attached to the carbon atoms. Labels include N(1), N(2), C(3), C(4), C(5), H(3), H(4), and H(5).</p>	 <p>Electrostatic potential map of Imidazole. The map shows the distribution of electron density, with red regions indicating electron-rich areas and blue regions indicating electron-poor areas. Labels include H(3) and H(4).</p>	 <p>Orbital density map of Imidazole. The map shows the distribution of electron density, with red and blue lobes representing different phases of the orbitals. Labels include N(1), H(7), and H(6).</p>
<p>Oxazole</p>	 <p>Ball-and-stick model of Oxazole (1,3,4-oxadiazole). The structure shows a five-membered aromatic ring with one oxygen atom (red) and three nitrogen atoms (blue). Hydrogen atoms (white) are attached to the carbon atoms. Labels include N(1), N(2), N(3), C(4), C(5), H(3), H(4), and H(5).</p>	 <p>Electrostatic potential map of Oxazole. The map shows the distribution of electron density, with red regions indicating electron-rich areas and blue regions indicating electron-poor areas. Labels include H(3) and H(4).</p>	 <p>Orbital density map of Oxazole. The map shows the distribution of electron density, with red and blue lobes representing different phases of the orbitals. Labels include H(7) and H(8).</p>
<p>Isoxazole</p>	 <p>Ball-and-stick model of Isoxazole (isoxazole). The structure shows a five-membered aromatic ring with one oxygen atom (red) and two nitrogen atoms (blue). Hydrogen atoms (white) are attached to the carbon atoms. Labels include N(1), N(2), C(3), C(4), C(5), H(3), H(4), and H(5).</p>	 <p>Electrostatic potential map of Isoxazole. The map shows the distribution of electron density, with red regions indicating electron-rich areas and blue regions indicating electron-poor areas. Labels include H(3), H(4), and H(5).</p>	 <p>Orbital density map of Isoxazole. The map shows the distribution of electron density, with red and blue lobes representing different phases of the orbitals. Labels include H(6), H(7), and H(5).</p>

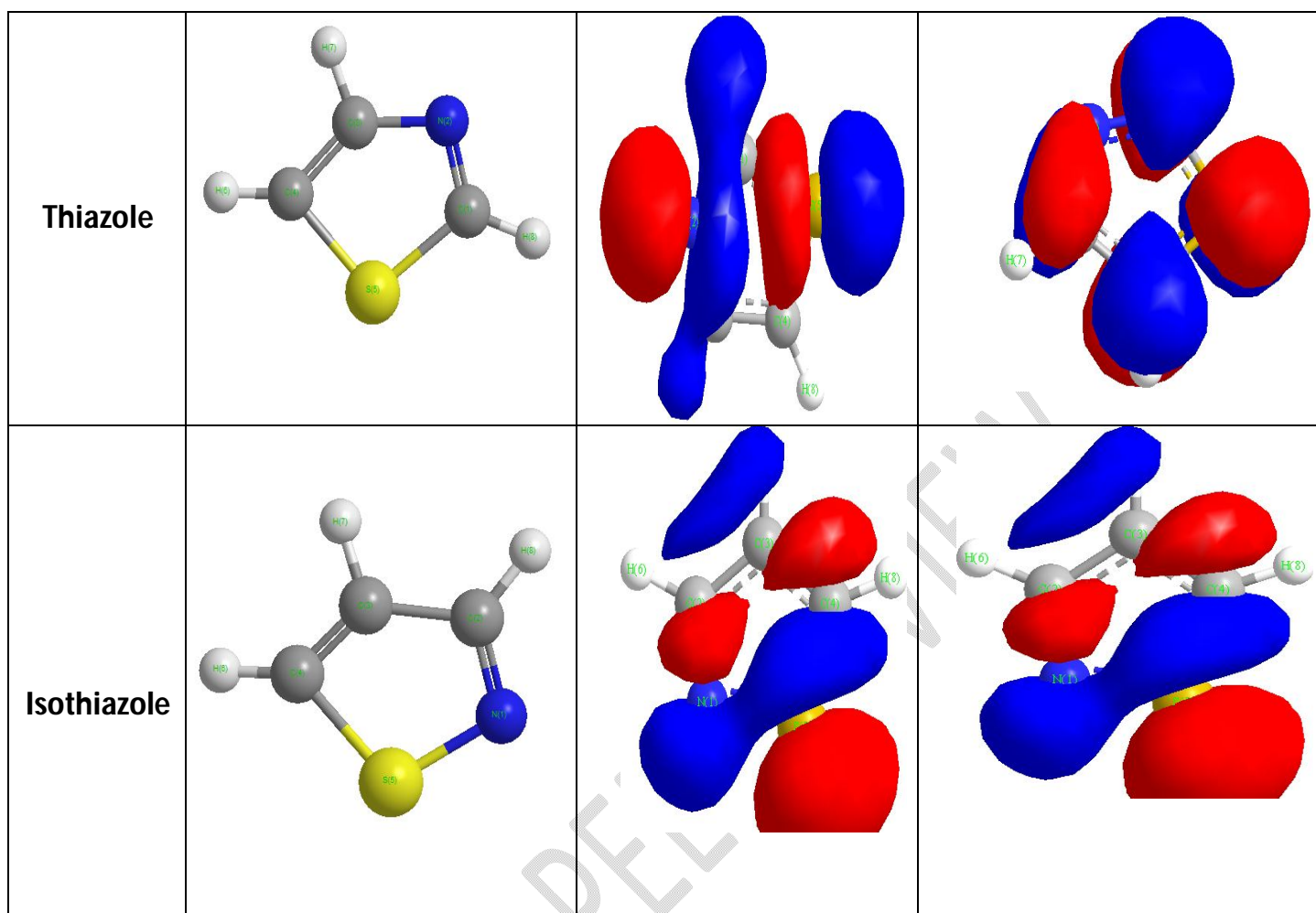


Table 3 Calculated quantum chemical parameters of inhibitors

Quantum parameter	Imidazole	Pyrazole	Oxazole	Isoxazole	Thiazole	Isothiazole
E_{HOMO}	-6.3598	-6.7286	-7.2616	-7.5438	-7.1346	-7.2614
E_{LUMO}	0.6522	0.3806	-0.4745	-0.9140	-1.0492	-1.2841
$\Delta E(\text{gap})$	007.01	7.1091	6.7871	6.6298	6.05854	5.9773
$I(\text{eV})$	6.3598	6.7286	7.2616	7.5438	7.1346	7.2614
$A(\text{eV})$	-0.6522	-0.3806	0.4745	0.9140	1.0492	1.2841
$X(\text{eV})$	2.8538	03.174	3.8680	4.2289	4.0919	4.2727
$\eta(\text{eV})$	03.506	3.5546	3.3935	3.3149	3.0427	2.9886

σ	0.2852	0.2813	0.2946	0.3016	0.3286	0.3346
ΔN	0.0282	0.0027	0.0185	0.0837	0.0758	0.0922
ω	1.1614	1.4117	2.2044	2.6974	2.7514	3.0542

$$X_{Al}= 3.2093 \quad , \quad \eta_{Al}= 2.7764$$

Soft molecules have small ΔE_{gap} whereas hard molecules have large ΔE_{gap} based on (Hard-Soft-Acid-Base)hypothesis (HSAB)[26,27]. The most effective inhibitor for the metals is classified as a soft base[28]. For this reason, the Isothiazole which has the smallest ΔE_{gap} and the highest softness (σ) is expected to have the best . This result is confirmed by calculating softness (σ) of the inhibitor and so its reactivity. Table 3 shows that the isothiazole has the highest value compared to the others. In addition, it can be observed (Table 3) that the hardness (η) of the Isot Thiazole has the smallest value of all fragments. This tendency is the reverse of what has been obtained for the softness (σ). Consequently, the Isothiazole is the best inhibitor. The electrophilicity index (ω) indicates the ability of the inhibitor to accept electrons from Aluminum.

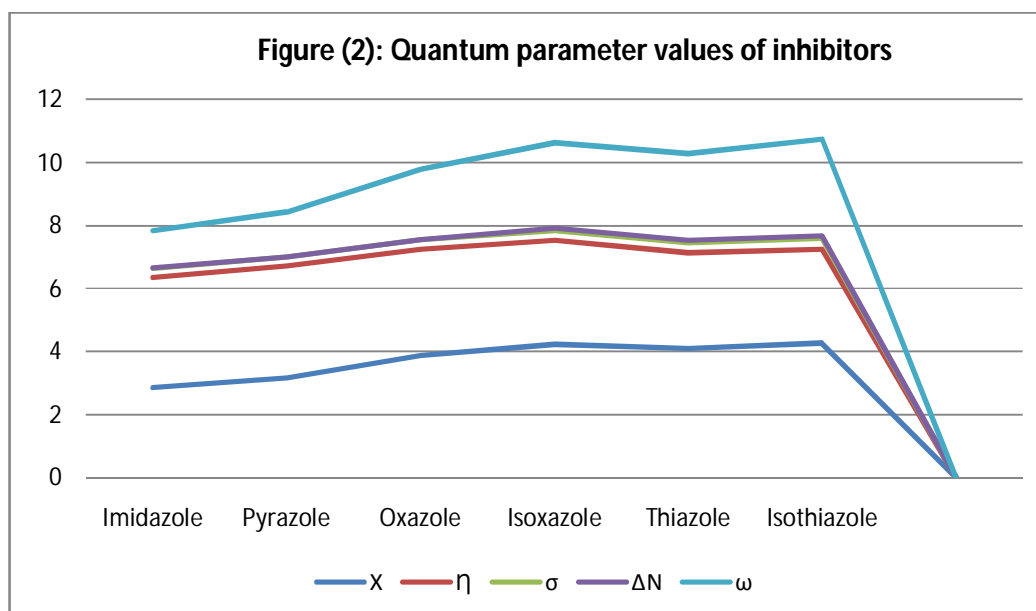
Compounds that can donate electrons to unoccupied orbital's of the metal surface to form coordinated covalent bonds and can also accept free electrons from the metal surface using their antibonding orbital's to form bonds and are excellent corrosion inhibitors.

CONCLUSIONS

Theoretical calculations gave a good picture of the compounds as aluminum corrosion inhibitors, and isothiazole showed greater inhibition efficiency compared to other inhibitors, as they were found to have higher values (ω) due to lower values of E_{LUMO} , which indicates their high acceptability. Electrons from aluminum.

The inhibition efficiency is increased due to the saturation and adsorption process on the aluminum surface, so the resulting inhibition efficiency order is





References

- [1]. Oguzie, E.E. Corrosion inhibition of aluminium in acidic and alkaline media by Sansevieria trifasciata extract. *Corros. Sci.* 2007, 49, 1527–1539.
- [2]. Sherif, E.M.; Park, S.M. Effects of 1,4-naphthoquinone on aluminum corrosion in 0.50 M sodium chloride solutions. *Electrochim. Acta* 2006, 51, 1313–1321.
- [3]. Osório, W.R.; Cheung, N.; Peixoto, L.C.; Garcia, A. Corrosion Resistance and Mechanical Properties of an Al 9wt% Si Alloy Treated by Laser Surface Remelting. *Int. J. Electrochem. Sci.* 2009, 4, 820–831.
- [4]. El-Shafei, A.A.; Moussa, M.N.H.; El-Far, A.A. Inhibitory effect of amino acids on Al pitting corrosion in 0.1 M NaCl. *J. Appl. Electrochem.* 1997, 27, 1075–1078.
- [5]. Xhanari, K.; Finsgar, M. Organic corrosion inhibitors for aluminium and its alloys in acid solutions: A review. *RSC Adv.* 2016, 6, 62833–62857.
- [6]. El-Meligi, A.A. Corrosion Preventive Strategies as a Crucial Need for Decreasing Environmental Pollution and Saving Economics. *Recent Pat. Corros. Sci.* 2010, 2, 22–33.
- [7]. Nnaji, N.J.N.; Ujam, O.T.; Ibisi, N.E.; Ani, J.U.; Onuegbu, T.O.; Olasunkanmi, L.O.; Ebenso, E.E. Morpholine and piperazine based carboxamide derivatives as corrosion inhibitors of mild steel in HCl medium. *J. Mol. Liq.* 2017, 230, 652–661.
- [8]. Umoren, S.A.; Eduok, U.M. Application of carbohydrate polymers as corrosion inhibitors for metal substrates in different media: A review. *Carbohydr. Polym.* 2016, 140, 314–341.

- [9]. Popoola, L.T.; Grema, A.S.; Latinwo, G.K.; Gutti, B.; Balogun, A.S. Corrosion problems during oil and gas production and its mitigation. *Int. J. Ind. Chem.* 2013, 4, 35.
- [10] Dewar, M.J.S.; Thiel, W., *J. Am. Chem. Soc.*, 1977, 99: 4899-4907.
- [11] Pearson, R.G., *Inorg. Chem.*, 1988, 27:734-740.
- [12] Parr, R.G.; Szentpaly, L.V.; Liu, S., *J. Am. Chem. Soc.*, 1999, 121: 1922-1924.
- [13] I. Lukovits, I.; E. Kalman, E.; F. Zucchi, F., *Corrosion*, 2001, 57: 3-8.
- [14] Parr, R.G.; Szentpaly, L.V.; Liu, S., *J. Am. Chem. Soc.*, 1999, 121: 1922-1924.
- [15] Pearson, R.G., *Inorg. Chem.*, 1988, 27:734-740.
- [16] Humpola, P.D.; Odetti, H.S.; Fertitta, A.E.; Vicente, J.L., *J. Chil. Chem. Soc.*, 2013; 58: 1541-1544.
- [17] Gece, G.; Bilgic, S., *Corros. Sci.*, 2009, 51:1876-1878.
- [18] D. R. Lide, *CRC Handbook of Chemistry and Physics*, 88th ed., 2007- 2008.
- [19] D. R. Lide, *CRC Handbook of Chemistry and Physics*, 88th ed., 2007- 2008.
- [20] S. Martinez, *Mater. Chem. Phys.* 77, 97 (2002).
- [21] A.Y. Musa, A.H. Kadhum, A.B. Rohoma, and H. Mesmari, *J. Mol. Struct.* **969**, 233 (2010).
- [22] G. Gece, S. Bilgic, *Corros. Sci.* **51**, 1876 (2009)
- [23] G. Klopman, *J. Am. Chem. Soc.*, 90, 233 (1968).
- [24] T. Arslan, F. Kandemirli, E. E. Ebenso, I. Love, H. Alemu, *Corros. Sci.*, **51**, 35 (2009).
- [25] . Li. S. Deng, H. Fu, T. Li, *Electrochim. Acta*, **54**, 4089 (2009)
- [26]. G. M. Al-Mazaideh, W. B. Ejlidi, S. M. Khalil, *Inter. Res. J. Pure & Appl. Chem.*, 2016, 12(4), 1.
- [27]. G. M. Al-Mazaideh, W. A. Al-Zereini, A. H. Al-Mustafa, S. M. Khalil, *Adv. Envi. Biol.*, 2016, 10 (8), 159.
- [28]. X. Li, S. Deng, H. Fu, T. Li, *Electrochem. Acta.*, 2009, 54(16), 4089.